Universiteit Leiden
The Netherlands

The development of molecular tools for investigating NAD+ metabolism and signalling
Minnee, H.

Chapter 3

A complete collection of ADP-ribosylated histidine isosteres through Cu(I)- and Ru(II)-catalyzed click chemistry

Introduction

Adenosine diphosphate ribosylation is a highly versatile and dynamic post-translational modification (PTM) in which the well-known redox co-factor nicotinamide dinucleotide adenine (NAD^{+}) is used to covalently link an adenosine diphosphate ribose (ADPr) molecule to a nucleophilic amino acid functionality. It is an ubiquitously expressed modification that allows spatiotemporal regulation of important cellular pathways including adipogenesis[1], DNA damage repair[2], gene expression[3] and apoptosis.[4] ADP ribosylation is effected by a family of (ADP-ribosyl)transferase enzymes termed PARPs.[5] Most members transfer a single ADPr moiety to a nucleophilic acceptor, which is referred to as mono-ADP-ribosylation (MARylation), although a small subset of PARPs (PARP1, 2, 5a and 5b) are able to mediate poly-ADP-ribosylation (PARylation) to create a linear polymer[6] with occasional branches.[7] The resulting poly-ADPr chains can be truncated by poly(ADP-ribosyl)glycohydrolase (PARG)[8,9] to yield a MARylated protein, after which a collection of (ADP-ribosyl)hydrolases and macrodomain proteins with distinct substrate specificity remove the final protein-linked ADPr moiety.[10–14]

The most common amino acid residue to be ADP-ribosylated is serine,[15,2,16] but glutamate, aspartate,[17–19,1] arginine[20], cysteine[15,21], lysine[22] and more recently tyrosine[23,15] and histidine[24,25] have been found to be ADP-ribosylated as well. Synthetic, well-defined MARylated peptides and ADPr-oligomers have been shown to be valuable molecular tools to investigate ADP-ribosylation, informing on the exact structure of ADPr polymers and modified peptides, the

chemical and enzymatic stability of the PTMs as well as the binding with interaction partners.[26–29] Various isosteres of ADP-ribosylated amino acids have been introduced as ADPr chemical biology tools with special attention being paid to stabilizing the glycosidic linkage that connects the ADPr-moiety to a protein and to expediate synthetic accessibility. Examples of the isosteric replacements for native ADPr-peptides include ADP-ribosylated glutamine and asparagine[30,31] and *N*-methyl aminooxy functionalized peptides[32] serving as base-stable substitutes for their glutamate and aspartate counterparts. Likewise, the urea functionality of citrulline has been introduced as a mimic for the guanidine group of arginine.[31] Click chemistry has been implemented to generate non-natural MARylated oligopeptides[33–35] and even full length proteins, as was demonstrated by the synthesis ADP-ribosylated ubiquitin, carrying the ADPr moiety at specific arginine residues.[36]

The imidazole ring of histidine has recently been identified as a potential ADP-ribosylation site.[24] Proteomics studies have however been unable to elucidate the nature of the ribosyl-histidine linkage. The imidazolyl side chain of histidine carries two possible modification sites that are commonly referred to as the N(π)- and N(τ)-positions (Figure 1). In addition, the chirality of the ribosyl anomeric center is unknown. Although all ADP-ribosyl linkages identified to date are α-configured (as a result of the substitution of nicotinamide at the anomeric centre of NAD$^+$ with inversion of stereochemistry), it cannot *a priori* be ruled out that the linkage to the histidine imidazolyl group is β-configured. For example, ADPr-Arg has been shown to spontaneously anomerise under physiological conditions via an endocyclic ring-opening pathway to transform the α-ribosyl linkage into the corresponding β-ribose.[37]
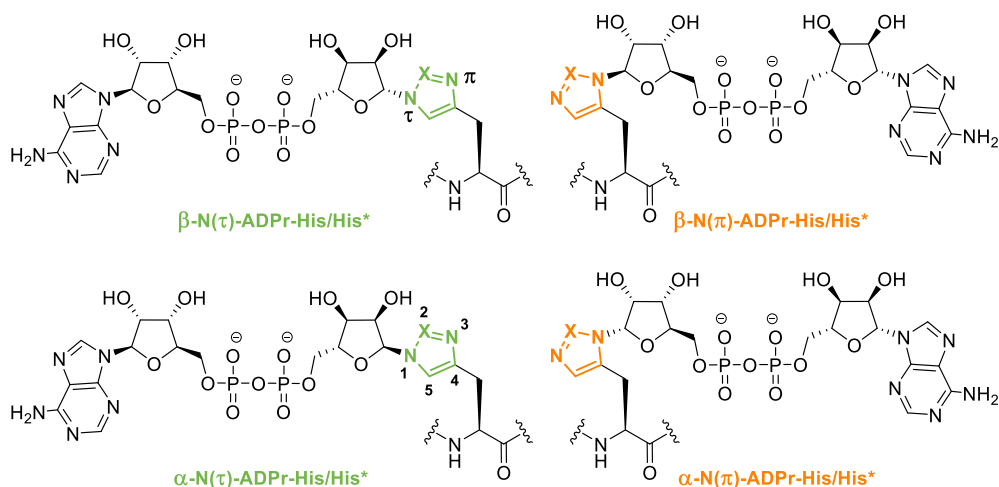
Figure 1| All four possible chemical structures for ADP-ribosylated histidine residues (X=CH), including the pros ('near', π) and tele ('far', τ) terminology for the imidazolium nitrogen atoms. The 1,4- and 1,5-disubstituted triazole-based isosteres (X=N, referred to as His*) mimic their N(τ)- and N(π)-ADP ribosylated histidine counterparts, respectively. Numbering nomenclature of triazolyl-functionalities is highlighted.

Chapter 2 reported on the synthesis of triazolyl-linked N(τ)-ADP-ribosylated conjugates that function as histidine isosteres, indicated here as N(τ)-ADPr-His* (Figure 1). These mimetics were generated via a convergent synthesis, introducing the 1,4-disubstituted triazole moieties by exploiting the highly regioselective Cu(I)-catalyzed azide-alkyne cycloaddition (CuAAC) of azido-ADPr derivatives to a propargyl glycine residue, pre-installed in the peptide chain by solid-phase peptide synthesis (SPPS).[35] In order to expand the toolbox to investigate ADPr-histidine biology, it was reasoned that the less common Ru(II)-catalyzed azide-alkyne cycloaddition (RuAAC)[38] could be exploited to access the missing α- and β-configured 1,5-triazole counterparts. Although the RuAAC has been successfully applied to peptides before,[39] it was incompatible with the late-stage conjugation of an azide-modified ADPr to an oligopeptide carrying an alkyne click handle due to degradation of the ADPr analogue observed by liquid-chromatography mass-spectrometry (LC-MS) analysis. Therefore, an alternative methodology towards the 1,5-disubstituted triazole-based isosteres for ADPr-histidine was required (Figure 2).
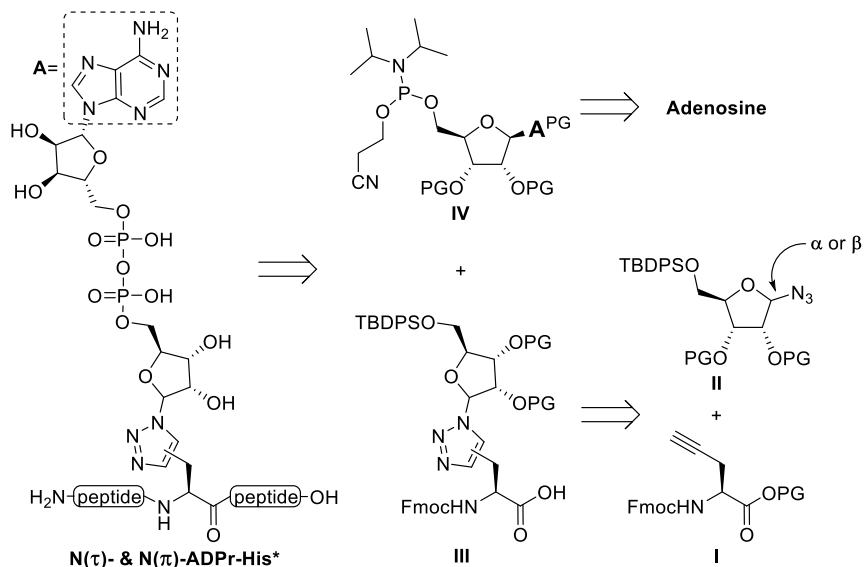
Figure 2 | Retrosynthetic analysis of 1,4- and 1,5-disubstituted triazole-based isosteres for N(τ)- and N(π)-ADP ribosylated histidine respectively, referred to as N(τ)- and N(π)-ADPr-His*. The peptide fragment HPF1$_{221-233}$ (T-F-H*-G-A-G-L-V-V-P-V-D-K, where H* refers to the triazole isostere) includes the histidine modification site that was recently identified in proteomic experiments.[24] Here, adenine is abbreviated as **A** and PG is used to depict an unspecified protecting group.

This chapter deals with the development of a stepwise SPPS approach to access both 1,4-triazoles, resembling N(τ)-ADPr-His, and 1,5-triazoles, mimicking the N(π)-ADPr-His, having either the α- or β-ribosyl configuration (Figure 2). A fluorenylmethyloxycarbonyl (Fmoc)-propargylglycine **I** was first conjugated to α- or β-configured azidoribose **II** using either

Cu(I)- or Ru(II)-catalyzed click chemistry to provide a comprehensive set of four distinct, SPPS-compatible building blocks **III** after removal of the corresponding carboxylic acid protecting group. The resulting key intermediates **III** could then be used in a SPPS protocol for the incorporation in a peptide fragment originating from histone PARylation factor 1 (HPF1), as the histidine residue in this peptide has been identified as a ribosylation site in recent proteomics studies,[24] through standard Fmoc-based peptide chemistry. Next, on resin phosphorylation and pyrophosphate formation following a well-established P(III)-P(V) coupling strategy[40] with suitably protected adenosine amidites **IV**, synthesized according to literature procedures from adenosine,[41,42] and a series of deprotection steps enabled the synthesis of the desired N(τ)- and N(π)-ADPr-His* mimetics. The resulting ADP-ribosylated conjugates have been used for stability studies to probe the integrity of the fragments under conditions typically used in proteomics work flows and were subsequently subjected to a panel of (ADP-ribosyl)hydrolases. These studies have revealed the 1,5-triazole analogues to be less stable under basic conditions and to be better substrates for ARH3 than their 1,4-counterparts.

Results and discussion

The preparation of 1,4- and 1,5-disubstituted triazole building blocks that are compatible with Fmoc-based SPPS commenced with the synthesis of β-configured azide **3**, which was derived from the commercially available ribose tetraacetate over four steps according to previously reported literature procedures (Scheme 1A).[35,43] The required propargylglycine could be accessed from Boc-Asp-OBn through a radical mediated decarboxylative alkynylation, as described by Baran and co-workers[44,45] for the synthesis of homo-propargylglycine from Boc-Glu-OBn.[46] To this end, Boc-Asp-OBn **4** was transformed in redox-active ester **5** via a Steglich esterification (Scheme 1A). Ethynylzinc chloride was prepared *in situ* from its Grignard precursor and an equimolar mixture of zinc chloride and lithium chloride in THF. To ensure the efficient and consistent formation of alkyne **6** it was found that the bipyridine-Ni(II) complex solution and a large excess of the ethynylzinc chloride had to be added to phthalimide **5** in quick succession. In this way the fully protected propargyl glycine **6** was obtained in 73% yield. Protecting group manipulations then provided Fmoc-propargylglycine benzyl ester **7**, which could be conjugated to β-configured azide **3** in a Cu(I)- or Ru(II)-catalyzed cycloaddition. Successive addition of CuSO₄ and sodium ascorbate to a solution containing equimolar amounts of azide **3** and propargylglycine **7** in DMF provided a single product (**8**) that was conveniently isolated by silica gel column chromatography. Formation of 1,4-disubstituted triazole **8** was confirmed using heteronuclear multiple bond correlation (HMBC) NMR spectroscopy, which revealed a clear coupling between the ribosyl H-1' and the tertiary C-5 of the triazole unit (Figure 3).

To generate the alternative 1,5-triazole, azide **3** was clicked to alkyne **7** using the chloro(pentamethylcyclo-pentadienyl)(cyclo octadiene)ruthenium (II) (Cp*RuCl(COD)) catalyst. An almost immediate conversion of the click partners **3** and **7** was realized by microwave heating the components in THF at 100 °C in the presence of the Cp*RuCl(COD) catalyst to

provide 1,5-triazole **10** in 85% yield.[47] The isolated product clearly differed from the previously isolated 1,4-regioisomer **8** according to both ^{1}H and ^{13}C NMR. HMBC measurements revealed a strong coupling between the ribosyl H-1' and the quaternary C-5 of the triazole moiety proving the regioselective formation of the 1,5-disubstituted triazole **10** (Figure 3). Deprotection of the benzyl esters in **8** and **10** provided the β-configured building blocks **9** and **11** for the planned Fmoc-based SPPS endeavors.
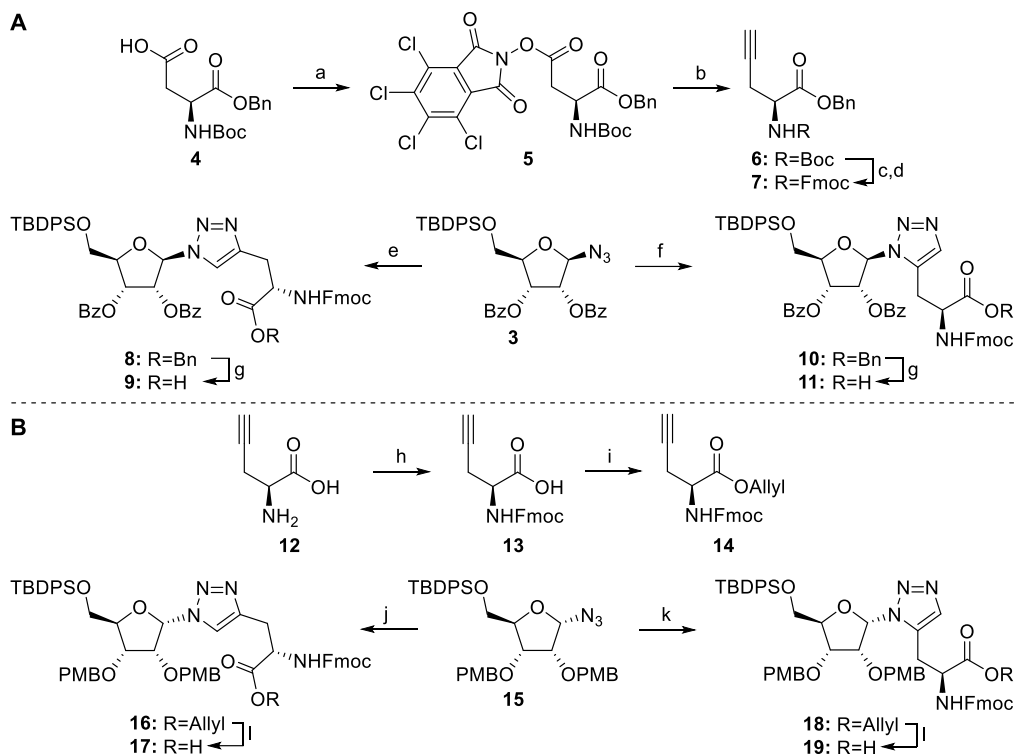

Scheme 1| Preparation of triazolyl-linked ribosylated building blocks through Cu(I)- and Ru(II)-catalyzed cycloadditions between suitably protected propargylglycine analogues with β-configured azido-ribofuranoside **3** (A) or α-configured azido-ribofuranoside **15** (B). Reagents and conditions: a) *N*-hydroxytetrachlorophthalimide, DCC, DMAP, DCM, rt, 16 h (81%). b) Ethynylmagnesium bromide, 4,4-dimethoxy-2,2′-bipyridine, NiCl$_2$, ZnCl$_2$, LiCl, THF/DMF (1:1), rt, 16 h (73%). c) TFA, DCM, rt, 2 h. d) Fmoc-OSu, NaHCO$_3$, H$_2$O/MeCN (1:1), rt, 16 h (91% over 2 steps). e) **7**, CuSO$_4$, sodium ascorbate, DMF, rt, 1 h (71%). f) **7**, Cp*RuCl(COD), THF, microwave, 100°C, 5 min (85%). g) H$_2$, Pd/C, MeOH, rt, 3.5 h (80% for **9**, 90% for **11**). h) Fmoc-OSu, NaHCO$_3$, H$_2$O/THF (1:1), rt, 16 h (quant). i) AllylOH, DMAP, DIC, DCM, rt, 45 min (81%). j) **14**, CuSO$_4$, sodium ascorbate, DMF, rt, 1 h (93%). k) **14**, Cp*RuCl(COD), THF, microwave, 100 °C, 1 h (60%). l) Pd(PPh$_3$)$_4$, DMBA, DCM, rt, 1.5 h (96% for **17**, 85% for **19**).

In the syntheses of the corresponding 1,4- and 1,5-triazole α-ribosyl building blocks, non-participating benzyl-type protecting groups are required to install the α-azido ribosyl linkages.

Therefore, benzyl ester **7** described above is not suitable for the synthesis of the triazole amino acids **17** and **19**, and instead an allyl ester was used to mask the amino acid carboxylate. Since glutamic acid allyl esters are not readily commercially available, the route described above for the benzyl ester could not be followed and the required building block **14** had to be generated

from propargyl glycine **12** (Scheme 1B). Introduction of the Fmoc group under basic conditions in a H$_2$O/THF solvent system gave carboxylic acid **13**, which was converted into **14** via a Steglich esterification with DIC/DMAP and allyl alcohol. α-Configured azide **15** was prepared as described previously[35] and both click partners could be joined by applying the same reaction conditions as discussed above to give 1,4-triazole **16** in a good yield. The RuAAC-reaction to generate the 1,5-regioisomer **18** required some optimization. Incomplete conversion of azide **15** was observed when a small excess of alkyne **14** (1.3 eq) was used and even when an extended reaction time (>1 h) was used, the yield did not exceed 35%. Using a 2-fold excess of alkyne **14** eventually led to the formation of 1,5-triazole **18** in a satisfactory yield of 60%. The regiochemistry in **16** and **18** was again substantiated by HMBC data. Removal of the allyl ester functionality in **16** and **18** was mediated using a catalytic amount of tetrakis(triphenylphosphine)palladium(0) in the presence of 1,3-dimethylbarbituric acid (DMBA) as allyl scavenger to provide the desired α-configured SPPS building blocks **17** and **19**. With both anomeric configurations of ribosylated 1,4- and 1,5-triazoles in hand, the next goal was to construct the set of target ADPr-His* peptides using SPPS.
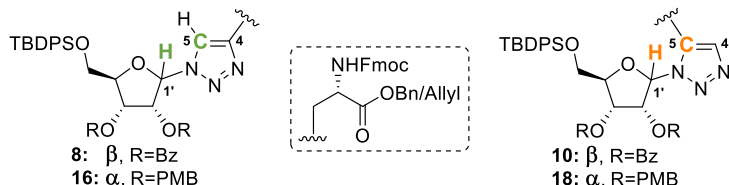
Figure 3. Characteristic proton-carbon three-bond couplings that have been observed in HMBC measurements for the here described 1,4- and 1,5-disubstituted triazoles building blocks are highlighted in green and orange respectively. No correlation between H-5 and C-1' was observed for any of the 1,4-triazoles in the acquired HMBC datasets.

As described above, peptides from histone PARylation factor 1 (HPF1), have been identified as ADP-ribosylation site in recent proteomic studies,[24] and these were thus assembled with the newly obtained 1,4- and 1,5-ribosylated building blocks.[35] Starting from Tentagel S AC resin, preloaded with *tert*-butyloxycarbonyl (Boc)-protected lysine, β-ribosyltriazolides **9** and **11** were incorporated using standard Fmoc-based SPPS conditions to provide fully protected intermediates **20A/B** (Scheme 2). Next, the installation of the pyrophosphate moiety was undertaken by unmasking the primary alcohol, appending the primary phosphate and extending this using a P(V)-P(III) coupling with a suitably protected adenosine phosphoramidite. Initially, removal of the silyl protecting group in **20A/B** with tetrabutylammonium fluoride (TBAF) in THF was explored,[48] but LC-MS analysis indicated that desilylation was accompanied by loss of

the 2'- and/or 3'-benzoyl moieties. This also implied that the C-terminal ester linkage to the resin might be at risk. Fortunately, HF-pyridine proved to be an adequate and milder alternative, leaving the ester functionalities unscathed while efficiently removing the TBDPS group. The liberated alcohol was phosphitylated with a 9-fluorenylmethyl (Fm) protected phosphoramidite[49] in the presence of 5-(ethylthio)-tetrazole (ETT) as activator. The resulting phosphite triester was subsequently oxidized with (1S)-(+)-(10-camphorsulfonyl)-oxaziridine (CSO) to provide protected phosphates **21A/B**. 1,8-Diazabicyclo[5.4.0]undec-7-ene (DBU) allowed for effective removal of the Fm-moieties, after which construction of the pyrophosphate was realized with adenosine amidite **30**[41] using P(III)-P(V) coupling chemistry under the *aegis* of ETT.[40] CSO mediated oxidation of the phosphate-phosphite intermediate into the pyrophosphate provided the immobilized and partially protected ADPr-peptides **22A/B**. After removal of the 2-cyanoethyl group with DBU, the solid support was treated with 50% trifluoroacetic acid (TFA) to ensure cleavage of the construct from the Tentagel resin while simultaneously removing the *t*-Bu and Boc protecting groups. Global deprotection of the remaining base sensitive groups was affected by treatment of the crude material with aqueous ammonia overnight and this was followed by purification using preparative HPLC (NH$_4$OAc buffered) to yield the β-configured N(τ)- and N(π)-ADPr-His* peptides **23** and **24** in 36% and 25% yield, respectively.

In a similar manner as described above, the α-configured building blocks **17** and **19** were incorporated in the peptide backbone, after which the resin-bound intermediates were desilylated with HF-pyridine and phosphorylated in a two-step fashion to give the Fm-phosphate triesters **26A/B**. After treatment with DBU, the liberated phosphate was coupled to fully Boc-protected adenosine amidite **31** to yield after oxidation, the immobilized and partially protected ADPr-peptides **27A/B**.[42] Elimination of the 2-cyanoethyl functionality in **27A/B**, was followed by treatment with TFA to simultaneously effect the removal of all remaining protecting groups and cleavage from the resin. Identical preparative HPLC conditions allowed for the isolation of the two remaining α-configured N(τ)- and N(π)-histidine isosteres **28** and **29**.

With all four ADPr-His* conjugates available, their stability under various conditions was evaluated in an LC-MS based assay. The conditions surveyed (NH$_2$OH, TFA and NaOH) were selected because of their frequent occurrence in ADP-ribosylome focused proteomics studies. In these studies NH$_2$OH elimination steps are implemented to identify acidic ADP-ribosylated residues[1,18], while basic conditions are applied for the pre-fractionation of peptides, which is generally followed by a subsequent acid treatment.[15,25] All four isosteres remained unaffected under the TFA (0.1 M) or NH$_2$OH (0.5 M) conditions for at least 24 h, as no sign of degradation was observed by LC-MS. After 24 h of 0.1 M NaOH treatment, LC-MS analysis showed additional peaks for the β-N(τ)-ADPr-His* **23** and α-N(τ)-ADPr-His* **28** peptides. These peaks (5% and 12%) corresponded to products having an identical mass as the parent compounds, indicating an isomerization reaction. As the newly formed peaks did not correspond to the anomeric counterparts of the starting compounds, it was assumed that these products originate from
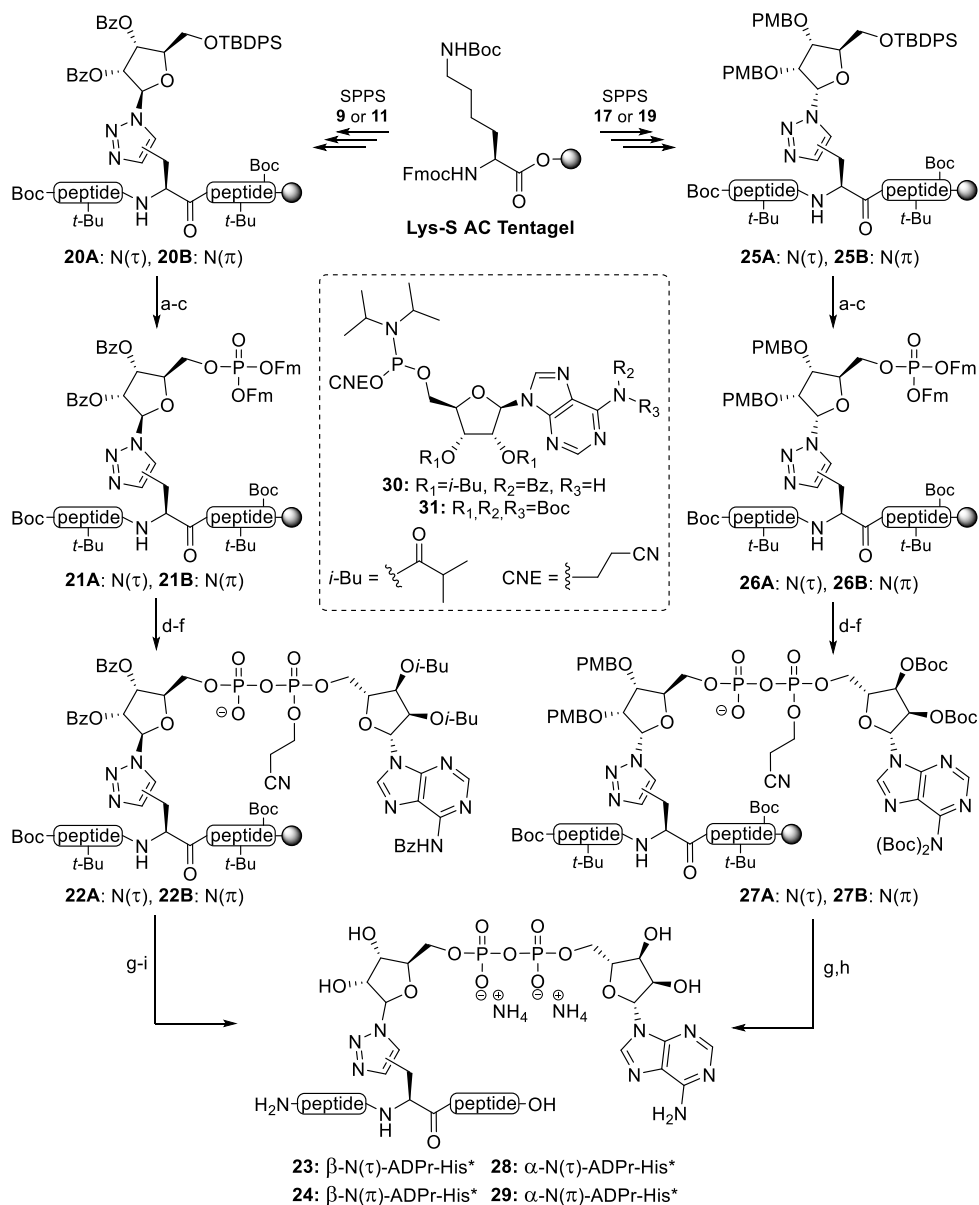
Scheme 2| Incorporation of ribosylated amino acids **9, 11, 17** and **19** in a peptide fragment originating from HPF1, resulting in (τ)- and (π)-His* isosteres in both α- and β-configuration. HPF1$_{221\text{-}233}$ sequence = T-F-H*-G-A-G-L-V-V-P-V-D-K, where H* refers to the triazole isostere. Reagents and conditions: a) HF-pyridine, pyridine, rt, 2x 45 min. b) (FmO)$_2$PN(i-Pr)$_2$, ETT, MeCN, rt, 30 min. c) CSO, MeCN, rt, 30 min. d) DBU, DMF, rt, 2x 15 min. e) **30** or **31**, ETT, MeCN, rt, 30 min. f) CSO, MeCN, rt, 30 min. g) DBU, DMF, rt, 2x 10 min. h) TFA, DCM, rt, 1 h (36% and 25% over 8 steps for **28** and **29** respectively). i) NH$_4$OH (28%), rt, 16 h (26% and 9% over 9 steps for **23** and **24** respectively).

epimerization of the His* α-carbon, as histidine has been observed to be relatively prone to epimerization. The steric hindrance in the more crowded 1,5-triazoles possibly makes these peptides more susceptible to the base-mediated epimerization than their 1,4-counterparts. The isomerization of the 1,5-triazoles β-N(π)-ADPr-His* **24** and α-N(π)-ADPr-His* **29** were monitored in a follow-up time course experiment (Figure 3A), showing rapid consumption of the starting peptides, leading after 12 h to a mixture of products in which 38% and 30% of the original peptides **24** and **29**, respectively were present.

Finally, the susceptibility of the peptides towards (ADP-ribosyl)hydrolase mediated hydrolysis was assessed (Figure 3B). Each of triazole conjugates **23, 24, 28** and **29** was incubated with a set of purified human (ADP-ribosyl)hydrolases. Any ADPr freed by the hydrolase in these reactions was converted by the NudT5 enzyme into adenosine monophosphate (AMP and quantified using the AMP-Glo assay (Promega).[50] As a positive control, the samples were treated with NudT16, which is able to hydrolyze the pyrophosphate linkage of both free and peptide-bound ADPr.[51] None of the hydrolases were able to cleave the *N*-glycosidic linkage of any of the four isosteres, except for ARH3, which was capable of hydrolyzing α-N(π)-ADPr-His* **29** and, albeit to a very minimal extent, α-N(τ)-ADPr-His* **28**,. Both β-anomers **23** and **24** remained unaffected by ARH3 under the given conditions. The slow but enzyme-dependent cleavage of α-N(τ)-ADPr-His* **28** is consistent with the hydrolysis described in the previous chapter (Chapter 2).[35]
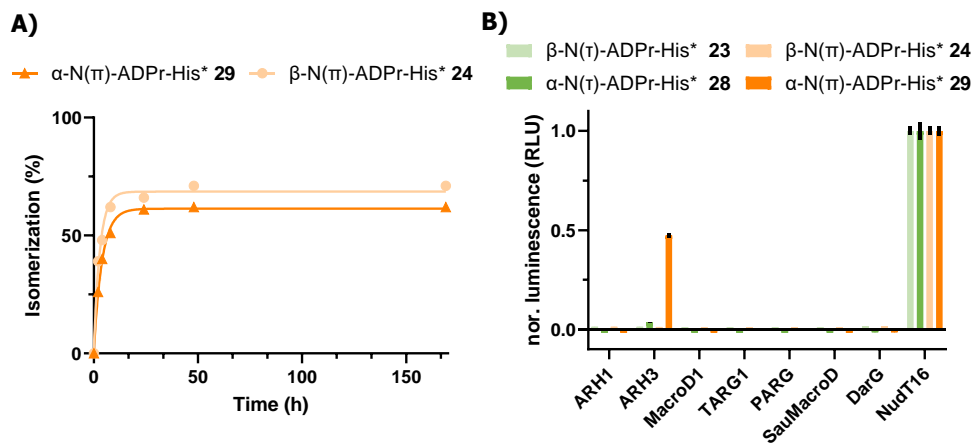
Figure 3| A) Chemical stability of 1,5-disubstitued triazoles **24** and **29** under basic conditions (NaOH, 0.1 M). Samples were extracted at different time points (2, 4, 8, 24, 48 and 169 h) and quenched with TFA prior to LC-MS injection. Peptide degradation was quantified by analyzing the UV-trace (260 nm) using Xcalibur software. Including an exponential one-phase decay trendline (R^2 values are 0.986 and 0.997 for **24** and **29** respectively). B) Enzymatic hydrolysis of the ribosyl linkages in ADP-ribosylated histidine peptides **23, 24, 28** and **29**. Enzymatic turnover of the various peptides was assessed by monitoring AMP release directly (NudT16) or converting released ADPr via NudT5 to AMP. AMP was measured using the AMP-Glo assay (Promega). Samples are background corrected and normalized to NudT16 activity.

Conclusion

A comprehensive SPPS-based methodology towards both 1,4- and 1,5-disubstituted triazole ADPr-peptide conjugates has been developed to mimic ADP ribosyl histidine peptides. To this end, the regioselectivity of Cu(I)- and Ru(II)-catalyzed click reactions has been exploited to join a propargyl glycine and an α- or β-configured azido ribosyl building block to furnish a complete set of both α- and β-configured N(τ)/N(π)-ADPr-His mimetics. Incorporation of these novel building blocks in a peptide sequence of interest was accomplished uneventfully using standard Fmoc-based SPPS conditions. Desilylation of the resulting resin-bound intermediates was performed with a slightly acidic HF-pyridine instead of TBAF, that has been employed previously,[53] to minimize the degradation of the ester linkages. The adenosine diphosphate moiety could be readily introduced through phosphoramidite chemistry to effectively deliver, after a sequence of deprotection steps, the target triazolyl peptide conjugates **23**, **24**, **28** and **29** in satisfactory to good yields. The stability of the peptides under nucleophilic (0.5 M NH_2OH), acidic (0.1 M TFA) and basic (0.1 M NaOH) conditions, commonly employed in ADP ribosyl proteomics protocols, was assessed, revealing the 1,5-triazoles to be sensitive to base-assisted epimerization. A NudT-based luminescent assay enabled the quantification of (ADP-ribosyl)hydrolase mediated degradation of the *N*-glycosidic linkage in the triazole constructs. Both α-N(τ)-ADPr-His* **28** and α-N(π)-ADPr-His* **29** proved to be susceptible to ARH3 mediated hydrolysis, with the 1,5-triazole **29** being significantly more labile than its 1,4-triazole counterpart **28**. These findings may suggest the α-N(π)-His to be the naturally occurring isomer, although the chemical stability studies also point to the intrinsic lability of the 1,5-triazole conjugates. These results warrant the development of synthetic methodology to access ADP ribosylated histidines, featuring the natural linkages, to determine whether the observed hydrolytic activity of ARH3 is of real biological relevance and applies to the natural imidazolyl-glycosidic linkages. It is expected that the methodology described here can be transposed to many other peptide sequences to effectively deliver ADPr-His* tools for (structural) biology purposes.

Experimental section

<u>Expression plasmids and protein purification</u>
The construction of the expression plasmids and the purification procedures were described earlier.[13,51,9,54] Briefly, expression plasmids were transferred into Rossetta (DE3) cells and grown at 37 °C to an OD$_{600}$ of 0.6 in LB medium supplemented with 1% (w/v) D-glucose and appropriate antibiotics. For (ADP-ribosyl)hydrolases (ARH1 and ARH3) the medium was further enriched by addition of 2 mM MgSO$_4$. Expression was induced with 0.4 mM isopropyl β-D-1- thioglactopyranoside (IPTG) and cultured were allowed to grow overnight at 17 °C. Cultures were harvested by centrifugation, pellets resuspended in lysis buffer (50 mM TrisHCl [pH 8], 500 mM NaCl and 25 mM imidazole) and stored at -20 °C until use. Proteins were purified by Ni^{2+}-NTA chromatography (Jena Bioscience) according to the manufacturer's protocol using the following buffers: all buffers contained 50 mM TrisHCl (pH 8) and 500 mM NaCl; additionally, the lysis buffer contained 25 mM, the washing buffer 40 mM, and the elution buffer 500 mM imidazole. Proteins were dialyzed overnight against 50 mM TrisHCl (pH 8), 200 mM NaCl, 1 mM dithiothreitol and 5% (v/v) glycerol and stored at -80 °C. For the purification of ARH1 and ARH3 all purification buffers were additionally supplemented with 10 mM MgCl$_2$.

<u>(ADP-ribosyl)hydrolase activity assay</u>
The peptide demodification assay was described earlier.[26,53] Briefly, peptide concentrations for the assay were estimated using absorbance at λ_{260nm} using the molar extinction coefficient of ADP-ribose (15,400 M^{-1} cm^{-1}). 10 μM indicated peptide were demodified by incubation with 0.5 μM hydrolase for 60 min at 30 °C in assay buffer (50 mM TrisHCl [pH 8], 200 mM NaCl, 10 mM MgCl2, 1 mM dithiothreitol and 0.2 μM human NUDT5)[26]. Reactions were stopped and analysed by performing the AMP-Glo™ assay (Promega) according to the manufacturer's protocol. Luminescence was recorded on a SpectraMax M5 plate reader (Molecular Devices) and data analysed with GraphPad Prism 7. Control reactions were carried out in absence of peptide.

<u>*General synthetic procedures*</u>
All chemicals were used as received unless stated otherwise. Dowex 50WX8 hydrogen form (100-200 mesh) was purchased at Sigma Aldrich and washed with H$_2$SO$_4$ (5 M, 3x) and MeOH (3x) prior to use. Molecular sieves were flamedried (3x) in vacuo before use. Solvents were dried over activated 4Å molsieves for 24 h except for MeCN and MeOH which were dried over 3Å molsieves. A solution of HCl (0.2 M in HFIP) was freshly prepared prior to the reaction by dissolving HCl (37%, 0.1 ml) to HFIP (5.9 ml). Reactions were performed under N$_2$ atmosphere unless stated otherwise. A Julabo FT902 cryostat was used for low temperature glycosylation reactions. Reaction mixtures were concentrated under reduced pressure using rotary evaporators at 40-45 ˚C unless state otherwise. Microwave syntheses were performed with the Biotage® Initiator+ microwave system using the 2.0-5.0 ml microwave vial types and the 'normal' absorption level setting. Reactions were monitored by thin layer chromatography (TLC) analysis using silica gel 60 F254 coated aluminum sheets from Merck. TLC plates were visualized with ultraviolet light (254 nm) or sprayed with H$_2$SO$_4$ (20% v/v in MeOH), potassium permanganate (1 g KMnO$_4$, 5 g K$_2$CO$_3$, in 200 ml H$_2$O) or ceric ammonium molybdate (1 g Ce(NH$_4$)$_4$(SO$_4$)$_4$•2H$_2$O, 2.5 g (NH$_4$)$_6$Mo$_7$O$_{24}$•4H$_2$O, 10 ml H$_2$SO$_4$ in 90 ml H$_2$O). Infrared (IR) values are reported in cm^{-1}. ^{1}H NMR, ^{13}C NMR and ^{31}P NMR spectra were recorded on Bruker AV-300 (300 mHz), AV-400 (400 mHz) or AV-500 (500 mHz) spectrometer. ^{13}C NMR spectra are acquired via the attached proton test (APT) experiment and are presented with even signals (C$_q$ and CH$_2$) pointing upwards and odd signals (CH and CH$_3$) pointing downwards. The chemical shifts are noted as δ-values in parts per million (ppm) relative to the tetramethylsilane signal (δ = 0 ppm) or solvent signal of

D_2O (δ = 4.79 ppm) for ^1H NMR and relative to the solvent signal of $CDCl_3$ (δ = 77.16 ppm) for ^{13}C NMR. Phosphorylation reactions were monitored with ^{31}P NMR using an acetone-D_6 insert for a locking signal and the resulting spectra were indirectly calibrated with H_3PO_4. HRMS samples were prepared in either MeOH, MeCN or milliQ grade H_2O with an approximate concentration of 1 mM and measured on a Thermo Scientific LTQ Orbitrap XL.

Solid phase peptide synthesis
Fmoc-Asp(*t*-Bu)-OH, Fmoc-Val-OH, Fmoc-Pro-OH, Fmoc-Leu-OH, Fmoc-Gly-OH, Fmoc-Ala-OH and Fmoc-Phe-OH were all obtained from Merck Novabiochem. Boc-Thr(tBu)-OH was acquired from BLD pharmatech GmbH. Lysine(Boc) was purchased pre-loaded on tentagel® S AC resin from RAPP Polymere GmbH.

The Fmoc-N-Ala-Gly-Leu-Val-Val-Pro-Val-Asp-Lys-S AC linked Tentagel® sequence was prepared using a Liberty Blue peptide synthesizer via 9-fluorenylmethoxycarbonyl (Fmoc) based solid phase peptide chemistry at a 250 µmol scale. A 4 fold excess of the amino acids relative to the resin loaded amino acid was added in each prolongation step. A total of 4 equivalents of the additives Diisopropylcarbodiimide (DIC) and OxymaPure were added simultaneously. The coupling was established in the microwave reaction chamber at 90 °C for 2.5 minutes. After each coupling the peptide was subjected three consecutive times to a 20 v/v% piperidine solution in DMF at 90 °C for 1 minute to remove the Fmoc protection group.

The Fmoc-N-Ala-Gly-Leu-Val-Val-Pro-Val-Asp-Lys-Tentagel® sequence was completed at a 50 µmol scale by hand in a fritted syringe. After each step the resin was rinsed with the corresponding solvent (3x 3 ml) unless stated otherwise. Fmoc protecting groups were removed by treatment with piperidine twice (10v/v% in DMF, 3 ml) for 3 and 7 min. Ribosylated amino acids **9**, **11**, **17** and **19** (0.1 mmol, 2 eq.) were coupled overnight in the presence DIPEA (40 µl, 4.5 eq.) and HCTU (0.1 mmol, 2 eq.) in DMF (3 ml). Fmoc-Phe-OH and Boc-Thr(*t*-Bu)-OH (0.25 mmol, 5 eq) were coupled for 45 min with HCTU (0.25 mmol, 5 eq) and DIPEA (90 µl, 10 eq.) in DMF (3 ml).

On-resin phosphorylation, pyrophosphate construction and final deprotection
TBDPS deprotection was achieved by treating the resin (50 µmol) with HF•pyridine (70 wt%, 1 ml) in pyridine (3 ml) twice for 45 min. The resin was washed with DMF (3x 3ml), DCM (3x 5 ml), Et_2O (3x 5 ml) and anhydrous MeCN (3x 3 ml) and flushed with nitrogen to minimize traces of water. Subsequently, the desilylated intermediate was treated with $(FmO)_2PN(i-Pr)_2$ (0.25 mmol, 5 eq.)[49] and ETT (0.25 mmol, 5 eq.) in anhydrous MeCN (3 ml) for 30 min. CSO (1 mmol, 20 eq.) in anhydrous MeCN (2 ml) was added and the resin was shaken again for 30 min. Then the newly introduced phosphate was deprotected with DBU (10v/v% in DMF, 2 ml) twice for 15 min and thoroughly washed with DCM (3x 5 ml), Et_2O (3x 5 ml) and anhydrous MeCN (3x 3 ml) before treating with either **30**[41] or **31**[42] (0.2 mmol, 4 eq.) in the presence of ETT (0.4 mmol, 8 eq.) in anhydrous MeCN (3 ml) for 30 min. The P(III)-P(V) intermediate was oxidized again with CSO (1 mmol, 20 eq.) in anhydrous MeCN (2 ml) for 30 min. The resin was subsequently shaken with DBU (10v/v% in anhydrous DMF, 2 ml) twice for 10 min each to remove the cyanoethyl group. The modified oligopeptide was cleaved from the resin using TFA/TIS/DCM (50:50:2.5, 4 ml) for 1 h. The solution was poured into a Falcon® tube containing ice cold Et_2O (40 ml) and the resulting suspension was centrifuged (5 min, 3000 RCF) using an Eppendorf centrifuge 5702 followed by removal of the supernatant. The partially protected precursors of **23** and **24** were stirred overnight in NH_4OH (28wt%, 8 ml) to remove benzoyl and *iso*-butyryl protecting groups, after which the solution was diluted with milliQ grade H_2O (5 ml) and washed with Et_2O (4x 10 ml). The H_2O fraction was collected, concentrated under reduced pressure and the resulting crude residues were subjected to preparative RP-HPLC (NH_4OAc buffered system). In contrast, crude residues of **28** and **29** were neutralized with NH_4OH (28wt%, 5 ml), diluted with milliQ

grade H_2O (5 ml) and washed with Et_2O (4x 10 ml). The water layer was then collected, concentrated under reduced pressure and subjected to preparative RP-HPLC.

### 1-Azido-2,3-bis-*O*-benzoyl-5-*O*-*tert*-butyldiphenylsilyl-β-D-ribofuranoside (3).
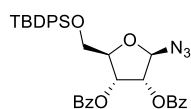
1-Azido-β-D-ribofuranoside[35,43] (7.0 g, 40 mmol) was co-evaporated with dioxane (3x) and dissolved in anhydrous pyridine (150 ml). TBDPSCl (15.0 ml, 56.0 mmol) was added and the reaction mixture was stirred overnight at rt. BzCl (14.0 ml, 120 mmol) was added and the yellow suspension was stirred for 2h before it was quenched with H_2O (5 ml). The mixture was diluted with EtOAc (150 ml) and washed with $NaHCO_3$ (sat., 3x 40 ml). The combined organic fractions were dried over $MgSO_4$, filtered and concentrated under reduced pressure. Purification of the crude residue by silica gel column chromatography (pentane/Et_2O = 85:15) provided title compound **3** (20.5 g, 33.0 mmol, 82%) as a clear oil. R_f = 0.5 (MeOH/DCM = 5:95). ^{1}H NMR (300 MHz, CDCl$_3$): δ 8.13 (dd, J = 13.6, 7.0 Hz, 4H), 8.04 – 7.77 (m, 4H), 7.66 – 7.33 (m, 12H), 6.14 (dd, J = 5.8, 4.4 Hz, 1H), 5.83 (d, J = 4.6 Hz, 2H), 4.71 (dt, J = 6.3, 3.4 Hz, 1H), 4.15 (ddd, J = 34.0, 11.5, 3.4 Hz, 2H), 1.32 (s, 9H). ^{13}C NMR (75 MHz, CDCl$_3$): δ 165.1, 164.9, 135.6, 135.6, 135.5, 135.5, 134.7, 133.4, 133.3, 132.7, 132.6, 129.8, 129.8, 129.7, 129.7, 129.6, 129.4, 129.0, 128.9, 128.3, 128.3, 127.8, 127.7, 127.7, 127.7, 127.6, 127.5, 93.0, 82.9, 75.4, 71.4, 63.3, 26.7, 26.5, 19.1. HRMS [$C_{35}H_{35}N_3O_6Si$ + NH_4]$^+$ = 639.26293 found, 639.26334 calculated; [$C_{35}H_{35}N_3O_6Si$ + Na]$^+$ = 644.21842 found, 644.21873 calculated.

Boc-L-Asp(*O*-hydroxyphtalamide)-OBn (5).
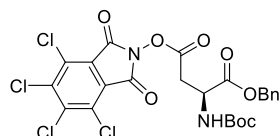
A solution of **4** (6.47 g, 20.0 mmol), *N*-hydroxy-tetrachlorophtalimide (7.28 g, 24.2 mmol) and DMAP (0.25 g, 2.0 mmol) in anhydrous DCM (200 ml) was purged with nitrogen. DIC (4.0 ml, 25.8 mmol) was added dropwise and the yellow suspension was stirred overnight at rt. The reaction mixture was filtered, washed with additional DCM and concentrated under reduced pressure. Purification of the crude residue by silica gel column chromatography (DCM/acetone = 97.5:2.5) yielded title compound **5** (9.86 g, 15.9 mmol, 80%) as a yellow solid. R_f = 0.4 (pentane/EtOAc = 80:20). ^{1}H NMR (300 MHz, CDCl$_3$): δ 7.40 – 7.29 (m, 5H), 5.52 (d, J = 8.0 Hz, 1H), 5.33 – 5.13 (m, 2H), 4.74 (dt, J = 8.4, 4.7 Hz, 1H), 3.32 (qd, J = 17.1, 4.9 Hz, 2H), 1.45 (s, 9H). ^{13}C NMR (75 MHz, CDCl$_3$): δ 169.7, 167.0, 157.2, 155.3, 141.2, 135.0, 130.6, 128.7, 128.6, 124.7, 68.1, 50.0, 34.1, 28.3. HRMS [$C_{24}H_{20}Cl_4N_3O_8$ + Na]$^+$ = 628.98345 found, 628.98371 calculated.

Boc-L-Pra-OBn (6).
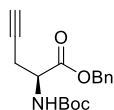
Nickel/ligand solution: NiCl·6H$_2$O (52 mg, 0.22 mmol) and 4,4-dimethoxy-2,2′-bipyridine (43 mg, 0.20 mmol) were dissolved in anhydrous DMF (10 ml) and stirred under argon atmosphere for 30 min prior to use.

Ethynylzinc chloride solution: a solution of ZnCl$_2$ (0.74 g, 5.4 mmol) and LiCl (0.24 g, 5.6 mmol) in anhydrous THF (5.5 ml) was stirred homogenous in a flame-dried round-bottom flask. Ethynylmagnesium bromide solution (0.5 M, 11 ml) was added and stirred for 30 minutes.

Compound **5** (0.62 g, 1.0 mmol) was co-evaporated with toluene and kept under argon atmosphere. The nickel/ligand solution (9.5 ml) and ethynylzinc chloride solution (11 ml) were added in quick succession and the resulting black mixture was stirred overnight. The reaction was quenched with HCl (1 M, 10 ml), diluted with H_2O (60 ml) and extracted with Et_2O (3x 50 ml). The combined organic fractions were washed with brine (3x 100 ml), dried over $MgSO_4$ and concentrated under reduced pressure. Purification of the crude residue by silica gel column chromatography (pentane/EtOAc = 90:10) yielded title compound **6**

(0.22 g, 0.74 mmol, 73%) as an off-white oil. R_f = 0.6 (pentane/EtOAc = 80:20). The obtained spectra were in full accordance with literature experimental data.[55]

Fmoc-L-Pra-OBn (7).
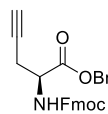
Compound **6** (0.38 g, 1.2 mmol) was dissolved in TFA/DCM (1:1, 6.1 ml) and stirred for 2h at rt. The yellow suspension was concentrated under reduced pressure and the crude residue was co-evaporated with toluene (3x) before dissolving in sat. NaHCO$_3$/MeCN (1:1, 12 ml). Fmoc-OSu (1.1 g, 3.0 mmol) was added and the reaction mixture was stirred overnight at rt. The yellow suspension was extracted with DCM (3x 50 ml). The combined organic fractions were washed with brine (3x 100 ml), dried over MgSO$_4$, filtered and concentrated under reduced pressure. Purification of the crude residue by silica gel column chromatography (pentane/EtOAc = 20:80) yielded title compound **7** (0.47 g, 1.1 mmol, 91%) as a white solid. **R_f** = 0.6 (pentane/Et$_2$O = 50:50). **^{1}H NMR** (500 MHz, CDCl$_3$) δ 7.72 (d, J = 7.5 Hz, 2H), 7.58 (d, J = 7.5 Hz, 2H), 7.39 − 7.24 (m, 10H), 5.76 (d, J = 8.3 Hz, 1H), 5.19 (q, J = 12.2 Hz, 2H), 4.58 (dt, J = 8.8, 4.8 Hz, 1H), 4.37 (d, J = 7.3 Hz, 2H), 4.20 (t, J = 7.2 Hz, 1H), 2.77 (dd, J = 5.0, 2.6 Hz, 2H), 2.01 (t, J = 2.5 Hz, 1H). **^{13}C NMR** (126 MHz, CDCl$_3$): δ 170.4, 155.8, 144.0, 143.9, 141.5, 135.3, 128.8, 128.7, 128.5, 127.9, 127.3, 125.3, 120.2, 78.5, 72.2, 67.8, 67.4, 52.7, 47.3, 22.9. **HRMS** [C$_{27}$H$_{23}$NO$_4$ + H]$^+$ = 426.16950 found, 426.16998 calculated; [C$_{27}$H$_{23}$NO$_4$ + NH$_4$]$^+$ = 443.19612 found, 443.19653 calculated; [C$_{27}$H$_{23}$NO$_4$ + Na]$^+$ = 448.15193 found, 448.15143 calculated.

Fmoc-His*(1'-N(τ)-2',3'-bis-O-benzoyl-5'-O-tert-diphenylsilyl-β-D-ribofuranosyl)-OBn (8).
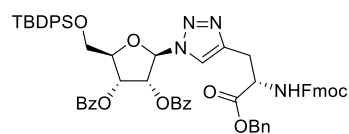
To a solution of **3** (0.19 g, 0.30 mmol) and **7** (0.10 g, 0.30 mmol) in DMF (3 ml) were added CuSO$_4$·5H$_2$O (75 mg, 0.30 mmol) and sodium ascorbate (0.18 g, 0.90 mmol) consecutively. The green suspension was stirred at rt for 1 h, diluted with H$_2$O (30 ml) and extracted with Et$_2$O (3x 20 ml). The combined organic fractions were washed with brine (1x 20 ml), dried over MgSO$_4$, filtered and concentrated under reduced pressure. Purification of the crude residue by silica gel column chromatography (pentane/EtOAc = 70:30) yielded title compound **8** (0.25 g, 0.24 mmol, 80%) as an off-white solid. **R_f** = 0.4 (pentane/EtOAc = 70:30). **^{1}H NMR** (500 MHz, CDCl$_3$): δ 8.00 − 7.89 (m, 4H), 7.77 − 7.70 (m, 2H), 7.67 (ddt, J = 8.2, 6.7, 1.6 Hz, 4H), 7.56 (tdd, J = 7.1, 3.5, 2.2 Hz, 3H), 7.55 − 7.48 (m, 2H), 7.43 − 7.23 (m, 20H), 6.46 (d, J = 5.2 Hz, 1H), 6.10 (t, J = 5.3 Hz, 1H), 6.04 (dd, J = 5.4, 4.1 Hz, 1H), 5.92 (d, J = 8.1 Hz, 1H), 5.21 − 5.10 (m, 2H), 4.69 (q, J = 6.3 Hz, 1H), 4.56 (d, J = 3.6 Hz, 1H), 4.36 (dd, J = 10.5, 7.3 Hz, 1H), 4.26 (dd, J = 10.5, 7.4 Hz, 1H), 4.19 (t, J = 7.4 Hz, 1H), 4.02 (d, J = 12.4 Hz, 2H), 3.25 − 3.08 (m, 2H), 1.12 (s, 9H). **^{13}C NMR** (126 MHz, CDCl$_3$): δ 170.9, 165.2, 164.9, 156.0, 144.0, 143.9, 143.2, 141.3, 141.2, 135.7, 135.5, 135.4, 133.7, 133.6, 133.0, 132.2, 130.1, 130.1, 129.9, 129.8, 129.0, 128.6, 128.6, 128.5, 128.5, 128.4, 128.4, 128.0, 127.7, 127.7, 127.1, 125.3, 125.3, 120.9, 119.9, 90.2, 84.2, 75.2, 71.8, 67.4, 67.3, 63.7, 53.5, 47.1, 29.7, 28.0, 27.0, 19.3. **HRMS** [C$_{62}$H$_{58}$N$_4$O$_{10}$Si + H]+ = 1047.39819 found, 1047.39950 calculated.

Fmoc-His*(1'-N(τ)-2',3'-bis-O-benzoyl-5'-O-tert-diphenylsilyl-β-D-ribofuranosyl)-OH (9).
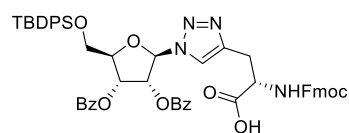
Compound **8** (2.8 g, 2.7 mmol) was dissolved in MeOH (54 ml) and purged with nitrogen for 15 minutes before adding Pd/C (10 wt%, 0.58 g, 0.50 mmol). The reaction mixture was bubbled with H$_2$ for 1 h and stirred overnight at rt under H$_2$ atmosphere. AcOH (0.5 ml) was added and the suspension was filtered over celite and washed with additional MeOH. The filtrate was concentrated under pressure and co-evaporated with toluene (3x). Purification of the crude residue by silica gel column chromatography (DCM/actone + 1% AcOH: 95:5)

yielded title compound **9** (2.06 g, 2.15 mmol, 80%) as a white foam. **R$_f$** = 0.3 (DCM/acetone + 1% AcOH = 90:10). **^{1}H NMR** (400 MHz, CDCl$_3$): δ 11.53 (bs, 1COOH), 7.92 (t, J = 7.5 Hz, 4H), 7.73 (s, 1H), 7.67 (d, J = 7.7 Hz, 6H), 7.58 − 7.40 (m, 4H), 7.39 − 7.19 (m, 14H), 6.51 (d, J = 4.8 Hz, 1H), 6.22 − 6.13 (m, 1H), 6.06 (t, J = 4.7 Hz, 1H), 4.70 (q, J = 6.0 Hz, 1H), 4.54 (q, J = 3.4 Hz, 1H), 4.32 (dd, J = 10.4, 7.4 Hz, 1H), 4.21 (dd, J = 10.4, 7.5 Hz, 1H), 4.13 (t, J = 7.2 Hz, 1H), 4.06 − 3.92 (m, 2H), 3.34 (qd, J = 15.3, 5.6 Hz, 2H), 1.12 (s, 9H). **^{13}C NMR** (101 MHz, CDCl$_3$): δ 173.1, 165.1, 164.8, 156.0, 143.8, 143.7, 143.0, 141.1, 141.0, 135.5, 135.4, 133.5, 132.7, 132.1, 130.0, 129.7, 129.6, 128.9, 128.7, 128.4, 128.3, 128.1, 127.9, 127.9, 127.5, 127.0, 125.2, 125.2, 121.8, 119.7, 90.3, 84.1, 75.2, 71.6, 67.0, 63.4, 53.3, 46.9, 27.6, 26.8, 19.1. **HRMS** [C$_{55}$H$_{52}$N$_4$O$_{10}$Si + H]$^+$ = 957.35206 found, 957.35255 calculated.

Fmoc-His*(1'-N(π)-2',3'-bis-*O*-benzoyl-5'-*O*-*tert*-diphenylsilyl-β-D-ribofuranosyl)-OBn (10).
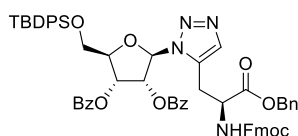

Compounds **3** (0.32 g, 0.50 mmol) and **7** (0.14 g, 0.32 mmol) were co-evaporated with toluene (3x) before dissolving in anhydrous THF (5 ml). The solution was purged with nitrogen gas for 15 min before adding C$_p$*RuCl(COD) (5 mg, 0.01 mmol). The yellow solution was heated to 100 °C in the microwave for 5 min and concentrated under reduced pressure. Purification of the crude residue by silica gel column chromatography (pentane/EtOAc = 60:40) yielded title compound **10** (0.30 g, 0.31 mmol, 85%) as a white solid. **R$_f$** = 0.5 (pentane/EtOAc = 70:30). **^{1}H NMR** (600 MHz, CDCl$_3$): δ 7.92 (ddd, J = 27.5, 8.1, 1.4 Hz, 4H), 7.72 (d, J = 7.6 Hz, 2H), 7.64 − 7.55 (m, 4H), 7.54 − 7.41 (m, 4H), 7.40 − 7.30 (m, 7H), 7.31 − 7.21 (m, 13H), 6.47 (d, J = 2.3 Hz, 1H), 6.32 (d, J = 3.3 Hz, 1H), 6.17 (t, J = 5.6 Hz, 1H), 5.67 (d, J = 7.4 Hz, 1H), 5.23 − 5.07 (m, 2H), 4.73 (q, J = 6.4 Hz, 1H), 4.59 (q, J = 5.0 Hz, 1H), 4.22 (ddd, J = 121.1, 10.6, 7.2 Hz, 2H), 4.03 (t, J = 7.2 Hz, 1H), 3.94 − 3.84 (m, 2H), 3.38 (dd, J = 71.8, 6.1 Hz, 2H), 1.02 (s, 9H). **^{13}C NMR** (151 MHz, CDCl3): δ 170.2, 165.2, 165.1, 155.7, 143.6, 143.5, 141.2, 135.6, 135.6, 134.6, 133.8, 133.6, 133.4, 133.0, 132.9, 132.9, 129.8, 129.8, 129.8, 129.7, 129.1, 128.8, 128.8, 128.7, 128.7, 128.5, 128.4, 127.8, 127.7, 127.7, 127.7, 127.1, 125.0, 120.0, 87.9, 84.1, 75.0, 72.2, 68.0, 67.2, 63.9, 53.2, 47.0, 26.7, 19.1. **HRMS** [C$_{62}$H$_{58}$N$_4$O$_{10}$Si + H]$^+$ = 1047.39920 found, 1047.39950 calculated.

Fmoc-His*(1'-N(π)-2',3'-bis-*O*-benzoyl-5'-*O*-*tert*-diphenylsilyl-β-D-ribofuranosyl)-OH (11).
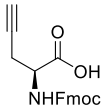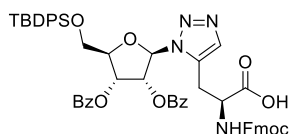

Compound **10** (5.0 g, 4.8 mmol) was dissolved in MeOH (95 ml) and purged with nitrogen for 15 minutes before adding Pd/C (10 wt%, 1.0 g, 0.90 mmol). The suspension was purged with H$_2$ and stirred overnight at rt overnight under H$_2$ atmosphere. AcOH (1 ml) was added and the reaction mixture was filtered over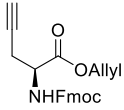 celite and washed with additional MeOH. The filtrate was concentrated under pressure. Purification of the crude residue by silica gel column chromatography (DCM/actone + 1% AcOH: 95:5) yielded title compound **11** (4.1 g, 4.3 mmol, 90%) as a yellowish foam. **R$_f$** = 0.3 (DCM/acetone + 1% AcOH = 90:10). **^{1}H NMR** (400 MHz, CDCl$_3$): δ 12.49 (bs, 1COOH), 7.91 (dd, J = 13.6, 7.7 Hz, 4H), 7.77 (s, 1H), 7.68 − 7.60 (m, 4H), 7.58 (d, 2H), 7.47 − 7.05 (m, 18H), 6.69 − 6.62 (m, 1H), 6.52 (d, J = 3.3 Hz, 1H), 6.25 (t, J = 5.4 Hz, 1H), 6.17 (d, J = 6.6 Hz, 1H), 4.77 (d, J = 6.5 Hz, 1H), 4.63 (q, J = 4.5 Hz, 1H), 4.31 − 4.22 (m, 1H), 4.11 − 3.83 (m, 4H), 3.58 (d, J = 11.9 Hz, 1H), 3.41 (d, J = 11.8 Hz, 1H), 1.04 (s, 9H). **^{13}C NMR** (101 MHz, CDCl$_3$) δ 172.5, 165.2, 156.0, 143.6, 143.6, 141.2, 135.6, 135.6, 134.4, 133.5, 133.4, 133.3, 132.8, 132.8, 129.8, 129.8, 129.8, 129.1, 129.0, 128.7, 128.4, 128.3, 127.8, 127.7, 127.2, 127.1, 125.3, 125.1, 119.9, 88.1, 84.2, 74.9, 72.0, 67.3, 63.7, 53.3, 46.9, 26.8, 25.9, 19.1. **HRMS** [C$_{55}$H$_{52}$N$_4$O$_{10}$Si + H]$^+$ = 957.35197 found, 957.35255 calculated.
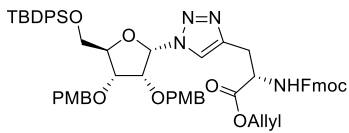
Fmoc-L-Pra-OH (13).

L-propargylglycine (150 mg, 1.33 mmol) and NaHCO$_3$ (278 mg, 3.32 mmol) were dissolved in milliQ water (7.4 ml). A solution of Fmoc-OSu (537 mg, 1.59 mmol) in THF (7.4 ml) was added to the reaction mixture and the suspension was stirred overnight at rt. The clear solution was acidified with HCl (1 M) until pH=1, diluted with H$_2$O (20 ml) and extracted with EtOAc (3x 30 ml). The combined organic fractions were washed with brine (30 ml), dried over MgSO$_4$, filtered and concentrated under reduced pressure. Purification of the crude residue by silica gel column chromatography (pentane/EtOAc + 1% AcOH= 80:20 → 60:40) yielded title compound **13** (445 mg, 1.33 mmol, quant.) as a white solid. **R$_f$** = 0.4 (pentane/EtOAc +1% AcOH = 50:50). The obtained spectra were in full accordance with literature experimental data.[56]

Fmoc-L-Pra-OAllyl (14).

To a suspension of **13** (250 mg, 0.745 mmol) and DMAP (18 mg, 0.15 mmol) in anhydrous DCM (7.5 ml) was added allyl alcohol (0.080 ml, 1.1 mmol) followed by DIC (1.0 M, 1.1 ml, 1.1 mmol). The resulting solution was stirred at rt for 45 min and concentrated under reduced pressure. Purification of the crude residue by silica gel column chromatography (Pentane/Et$_2$O = 95:5 → 90:10) yielded title compound **14** (228 mg, 0.601 mmol, 81%) as a white solid. **R$_f$** = 0.5 (Pentane/EtOAc = 80:20). **^{1}H NMR** (300 MHz, CDCl$_3$): δ 7.75 (d, J = 7.5 Hz, 2H), 7.60 (d, J = 7.4 Hz, 2H), 7.44 – 7.24 (m, 4H), 6.00 – 5.81 (m, 1H), 5.72 (d, J = 8.3 Hz, 1H), 5.40 – 5.20 (m, 2H), 4.77 – 4.61 (m, 2H), 4.65 – 4.46 (m, 1H), 4.39 (d, J = 7.2 Hz, 2H), 4.23 (t, J = 7.2 Hz, 1H), 2.80 (dd, J = 4.9, 2.7 Hz, 2H), 2.07 (t, J = 2.6 Hz, 1H). **^{13}C NMR** (75 MHz, CDCl$_3$): δ 170.0, 155.7, 143.8, 143.7, 141.3, 131.4, 127.8, 127.1, 125.2, 120.0, 119.0, 78.3, 72.0, 67.3, 66.4, 52.4, 47.1, 22.8. **HRMS** [C$_{23}$H$_{21}$NO$_4$ + H]$^+$ = 376.15406 found, 376.15433 calculated; [C$_{23}$H$_{21}$NO$_4$ + NH$_4$]$^+$ = 393.18088 found, 393.18058 calculated; [C$_{23}$H$_{21}$NO$_4$ + Na]$^+$ = 398.13628 found, 398.13602 calculated.

Fmoc-His*(1'-N(τ)-2',3'-bis-*O*-para-methoxybenzyl-5'-*O*-*tert*-diphenylsilyl-α-D-ribo-furanosyl)-OAllyl (16).

To a solution of **15**[35] (750 mg, 1.15 mmol) and **14** (560 mg, 1.49 mmol) in DMF (11.5 ml) were added CuSO$_4$·5H$_2$O (0.14 g, 0.57 mmol) and sodium ascorbate (0.68 g, 3.4 mmol) consecutively. The green suspension was stirred for 30 min at rt, diluted with water (100 ml) and extracted with Et$_2$O (3x 100 ml). The combined organic fractions were dried over MgSO$_4$, filtered and concentrated under reduced pressure. Purification of the crude residue by silica gel column chromatography (pentane/EtOAc = 90:10 → 70:30) yielded title compound **16** (1.10 g, 1.07 mmol, 93%) as a white foam. **R$_f$** = 0.6 (pentane/EtOAc = 60:40). **^{1}H NMR** (400 MHz, CDCl$_3$): δ 8.08 (s, 1H), 7.72 (d, J = 8.5 Hz, 2H), 7.65 – 7.54 (m, 6H), 7.47 – 7.32 (m, 8H), 7.27 (d, J = 1.2 Hz, 2H), 7.17 (d, J = 8.6 Hz, 2H), 7.03 (d, J = 8.6 Hz, 2H), 6.82 (dd, J = 19.4, 8.6 Hz, 4H), 6.55 (d, J = 6.0 Hz, 1H), 6.10 (d, J = 8.4 Hz, 1H), 5.90 – 5.75 (m, 1H), 5.29 – 5.13 (m, 2H), 4.75 (dt, J = 8.4, 5.3 Hz, 1H), 4.65 (d, J = 11.2 Hz, 1H), 4.63 – 4.52 (m, 2H), 4.53 – 4.43 (m, 2H), 4.41 – 4.18 (m, 5H), 4.24 – 4.16 (m, 2H), 3.77 (s, 3H), 3.77 – 3.69 (m, 4H), 3.58 (dd, J = 11.5, 2.4 Hz, 1H), 3.29 (d, J = 5.4 Hz, 2H), 0.99 (s, 9H). **^{13}C NMR** (101 MHz, CDCl$_3$): δ 170.8, 159.5, 159.5, 156.0, 143.9, 143.8, 142.3, 141.2, 141.2, 135.5, 135.4, 132.8, 132.4, 131.6, 129.9, 129.7, 129.4, 129.4, 128.7, 127.8, 127.6, 127.1, 125.3, 125.3, 123.3, 119.9, 119.8, 118.7, 113.9, 113.9, 113.8, 89.0, 85.0, 77.3, 76.6, 72.6, 72.5, 67.3, 66.0, 63.8, 55.2, 55.2, 53.7, 47.0, 28.1, 26.8, 19.1. **HRMS** [C$_{60}$H$_{64}$N$_4$O$_{10}$Si + H]$^+$ = 1029.44582 found, 1029.44645 calculated; [C$_{60}$H$_{64}$N$_4$O$_{10}$Si + Na]$^+$ = 1051.42797 found, 1051.42839 calculated.

Fmoc-His*(1'-N(τ)-(2',3'-bis-*O*-para-methoxybenzyl-5'-*O*-*tert*-diphenylsilyl-α-D-ribo-furanosyl)-OH (17).
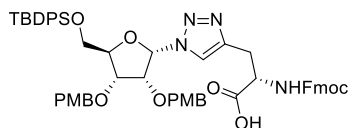

Compound **16** (1.10 g, 1.07 mmol) and DMBA (0.18 g, 1.2 mmol) were co-evaporated with toluene (3x) before dissolving in anhydrous DCM (22 ml). The solution was purged with argon for 15 min before adding Pd(PPh₃)₄ (25 mg, 0.021 mmol). After 1.5 h, the yellow solution was diluted with DCM (100 ml) and washed with citric acid (10wt%, 2x 100 ml). The H₂O layer was back-extracted with DCM (2x 75 ml. The combined organic fractions were dried over MgSO₄, filtered and concentrated under reduced pressure. Purification of the crude residue by silica gel column chromatography (DCM/acetone + 1% AcOH = 95:5 → 90:10) yielded title compound **17** (1.01 g, 1.02 mmol, 96%) as a white foam. R_f = 0.3 (DCM/acetone + 1% AcOH = 90:10). **¹H NMR** (400 MHz, CDCl₃): δ 10.92 (bs, COOH), 8.21 (s, 1H), 7.72 – 7.61 (m, 2H), 7.64 – 7.44 (m, 6H), 7.45 – 7.17 (m, 10H), 7.14 (d, J = 8.2 Hz, 2H), 7.02 (d, J = 8.2 Hz, 2H), 6.80 (dd, J = 20.2, 8.6 Hz, 2H), 6.53 (d, J = 5.9 Hz, 1H), 6.11 (d, J = 7.1 Hz, 1H), 4.74 (q, J = 5.9 Hz, 1H), 4.60 (d, J = 11.4 Hz, 1H), 4.52 – 4.39 (m, 2H), 4.38 – 4.27 (m, 3H), 4.22 – 4.07 (m, 4H), 3.76 – 3.63 (m, 7H), 3.58 – 3.52 (m, 1H), 3.47 – 3.40 (m, 2H), 0.97 (s, 9H). **¹³C NMR** (101 MHz, CDCl₃): δ 172.9, 159.4, 159.4, 156.0, 143.9, 143.8, 142.0, 141.1, 135.5, 135.4, 132.8, 132.3, 132.2, 132.1, 132.1, 132.0, 129.9, 129.5, 129.2, 128.6, 128.6, 128.5, 127.8, 127.8, 127.5, 127.5, 127.1, 127.0, 125.3, 125.2, 124.2, 119.7, 113.9, 113.8, 113.8, 89.3, 84.9, 76.4, 72.5, 72.4, 67.1, 63.6, 55.1, 55.1, 53.6, 46.9, 27.9, 26.7, 19.0. **HRMS** [$C_{57}H_{60}N_4O_{10}Si$ + H]⁺ = 989.41437 found, 989.41515 calculated.

Fmoc-His*(1'-N(π)-(2',3'-bis-*O*-para-methoxybenzyl-5'-*O*-*tert*-diphenylsilyl-α-D-ribo-furanosyl))-OAllyl (18).
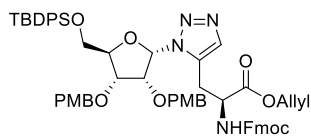

Compound **15** (1.07 g, 1.64 mmol) and **14** (1.23 g, 3.27 mmol) were co-evaporated with toluene (3x) before dissolving in anhydrous THF (25 ml). The solution was purged with argon gas for 15 min before adding Cₚ*RuCl(COD) (31 mg, 0.082 mmol). The yellow solution was heated to 100 °C in the microwave for 1 h and concentrated under reduced pressure. Purification of the crude residue by silica gel column chromatography (pentane/EtOAc = 90:10 → 70:30) yielded title compound **18** (1.01 g, 0.981 mmol, 60%) as a yellowish foam. R_f = 0.5 (pentane/EtOAc = 60:40). **¹H NMR** (500 MHz, CDCl₃): δ 7.72 (d, J = 7.5 Hz, 2H), 7.62 (td, J = 7.8, 1.5 Hz, 4H), 7.57 (s, 1H), 7.47 (dd, J = 13.1, 7.5 Hz, 2H), 7.42 – 7.21 (m, 10H), 7.15 (d, J = 8.4 Hz, 2H), 6.95 (d, J = 8.1 Hz, 2H), 6.80 (dd, J = 25.3, 8.6 Hz, 4H), 6.69 (d, J = 3.9 Hz, 1H), 5.82 – 5.70 (m, 1H), 5.65 (d, J = 8.2 Hz, 1H), 5.27 – 5.14 (m, 2H), 4.61 – 4.41 (m, 4H), 4.38 (dd, J = 7.6, 4.6 Hz, 1H), 4.35 – 4.29 (m, 2H), 4.26 (d, J = 7.4 Hz, 2H), 4.11 (t, J = 7.2 Hz, 1H), 4.05 – 3.92 (m, 3H), 3.81 – 3.68 (m, 7H), 3.45 (dd, J = 15.6, 8.9 Hz, 1H), 3.28 (dd, J = 15.5, 6.0 Hz, 1H), 1.02 (s, 9H). **¹³C NMR** (126 MHz, CDCl₃): δ 171.0, 159.6, 159.5, 155.7, 143.8, 143.7, 141.2, 141.2, 135.6, 135.5, 134.8, 134.3, 133.1, 132.6, 131.3, 129.9, 129.9, 129.8, 129.5, 129.2, 128.6, 127.8, 127.7, 127.2, 127.1, 125.1, 119.9, 119.0, 113.9, 113.9, 91.9, 82.4, 77.2, 76.2, 72.9, 72.5, 67.1, 66.1, 62.6, 55.2, 55.2, 53.6, 47.0, 26.9, 26.2, 19.2. **HRMS** [$C_{60}H_{64}N_4O_{10}Si$ + H]⁺ = 1029.44563 found, 1029.44645 calculated; [$C_{60}H_{64}N_4O_{10}Si$ + Na]⁺ = 1051.42816 found, 1051.42839 calculated.

Fmoc-His*(1'-N(π)-(2',3'-bis-*O*-para-methoxybenzyl-5'-*O-tert*-diphenylsilyl-α-D-ribo-furanosyl))-OH (19).
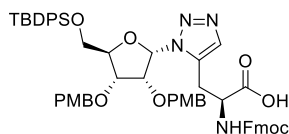
A solution of **18** (1.75 g, 1.70 mmol) and DMBA (0.29 g, 1.9 mmol) in anhydrous DCM (22 ml) was purged with argon for 15 min before adding Pd(PPh$_3$)$_4$ (39 mg, 0.034 mmol). After 1.5 h, the yellow solution was diluted with DCM (100 ml) and washed with citric acid (10wt%, 2x 100 ml). The H$_2$O layer was back-extracted with DCM (2x 75 ml. The combined organic fractions were dried over MgSO$_4$, filtered and concentrated under reduced pressure. Purification of the crude residue by silica gel column chromatography (DCM/acetone + 1% AcOH = 97.5:2.5 → 95:5) yielded title compound **19** (1.43 g, 1.45 mmol, 85%) as yellowish foam. **R$_f$** = 0.4 (DCM/acetone + 1% AcOH = 90:10). **^{1}H NMR** (500 MHz, CDCl$_3$): δ 9.76 (bs, COOH), 7.69 (d, *J* = 7.6 Hz, 2H), 7.66 − 7.56 (m, 5H), 7.51 − 7.44 (m, 2H), 7.44 − 7.35 (m, 2H), 7.36 − 7.27 (m, 6H), 7.26 − 7.17 (m, 2H), 7.12 (d, *J* = 8.2 Hz, 2H), 6.94 (d, *J* = 8.3 Hz, 2H), 6.77 (dd, *J* = 22.6, 8.6 Hz, 4H), 6.62 (d, *J* = 3.4 Hz, 1H), 5.77 (d, *J* = 7.9 Hz, 1H), 4.60 (q, *J* = 7.4 Hz, 1H), 4.52 (d, *J* = 6.7 Hz, 1H), 4.40 (d, *J* = 11.5 Hz, 1H), 4.33 − 4.22 (m, 5H), 4.13 − 4.03 (m, 2H), 4.02 − 3.92 (m, 2H), 3.73 (s, 3H), 3.69 (s, 4H), 3.53 − 3.45 (m, 1H), 3.37 (dd, *J* = 15.6, 6.1 Hz, 1H), 1.00 (s, 9H). **^{13}C NMR** (126 MHz, CDCl$_3$): δ 173.5, 159.5, 159.5, 155.9, 143.8, 141.2, 141.2, 135.7, 135.6, 135.5, 135.2, 133.0, 132.6, 132.3, 132.3, 132.2, 132.1, 129.9, 129.5, 129.2, 128.7, 128.6, 128.6, 127.8, 127.7, 127.7, 127.2, 127.1, 125.2, 125.1, 119.9, 113.9, 113.9, 91.8, 82.6, 77.1, 76.1, 72.8, 72.4, 67.1, 62.9, 55.2, 55.2, 53.4, 47.0, 26.9, 26.3, 19.2. **HRMS** [C$_{57}$H$_{60}$N$_4$O$_{10}$Si + H]$^+$ = 989.41477 found, 989.41515 calculated.

β-N(τ)-ADPr-His*: TF[H*]GAGLVVPVDK (H* = Triazolyl ADPr) (23).
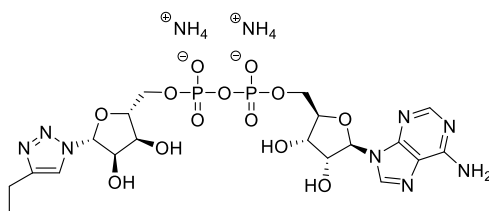
Title compound **23** was synthesized according to the general resin based procedure described above on a 50 µmol scale by incorporating the 1,4-disubstituted triazole **9**. The 5'-phosphoryl-ribofuranose intermediate was coupled to adenosine amidite **30**.[41] Purification of the crude residue (50 µmol) by preparative HPLC (NH$_4$OAc buffer) and subsequent lyophilization yielded title compound **23** (24.7 mg, 13.1 µmol, 26%) as a fluffy white powder. The obtained spectra were in full accordance with previously reported experimental data.[35] **LC-MS** R$_t$ = 5.30 min (10-50% MeCN/H$_2$O, TFA). **^{1}H NMR** (400 MHz, D$_2$O): δ 8.44 (s, 1H), 8.17 (s, 1H), 8.03 (s, 1H), 7.24 − 7.11 (m, 3H), 7.04 (d, *J* = 7.2 Hz, 2H), 6.01 (dd, *J* = 7.8, 5.2 Hz, 2H). **^{31}P NMR** (162 MHz, D$_2$O): δ -10.51, -10.63, -10.73, -10.86. **HRMS** [C$_{76}$H$_{118}$N$_{22}$O$_{30}$P$_2$ + 2H]$^{2+}$ = 941.39999 found, 941.40025 calculated; [C$_{76}$H$_{118}$N$_{22}$O$_{30}$P$_2$ + 3H]$^{3+}$ = 627.93600 found, 627.93592 calculated.

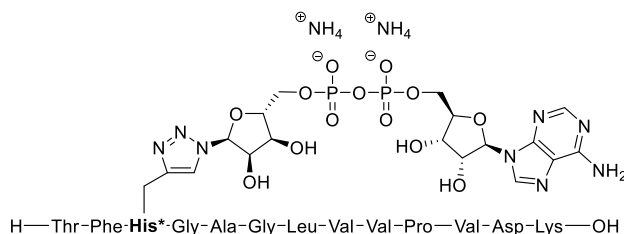## β-N(π)-ADPr-His*: TF[H*]GAGLVVPVDK (H* = Triazolyl ADPr) (24).
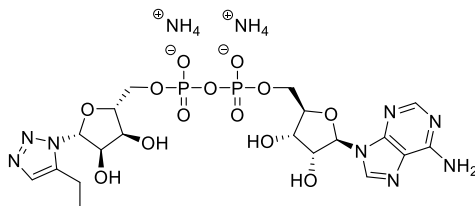
Title compound **24** was synthesized according to the general resin based procedure described above on a 50 µmol scale by incorporating the 1,4-disubstituted triazole **11**. The 5'-phosphoryl-ribofuranose intermediate was coupled to adenosine amidite **30**.[41] Purification of the crude residue

(50 µmol) by preparative HPLC (NH₄OAc buffer) and subsequent lyophilization yielded title compound **24** (8.0 mg, 4.3 µmol, 9%) as a fluffy white powder. **LC-MS** R_t = 4.41 min (10-50% MeCN/H₂O, TFA). **¹H NMR** (400 MHz, D₂O): δ 8.44 (s, 1H), 8.19 (s, 1H), 7.49 (s, 1H), 7.25 − 7.17 (m, J = 6.9, 6.5 Hz, 3H), 7.10 (d, J = 7.2 Hz, 2H), 6.04 (d, J = 5.5 Hz, 1H), 5.92 (d, J = 3.8 Hz, 1H). **³¹P NMR** (162 MHz, D₂O): δ -10.67. **HRMS** $[C_{76}H_{118}N_{22}O_{30}P_2 + 2H]^{2+}$ = 941.40000 found, 941.40025 calculated; $[C_{76}H_{118}N_{22}O_{30}P_2 + 3H]^{3+}$ = 627.93619 found, 627.93592 calculated.

α-N(τ)-ADPr-His*: TF[H*]GAGLVVPVDK (H* = Triazolyl ADPr) (28).

H⎯⎯Thr-Phe-**His***-Gly-Ala-Gly-Leu-Val-Val-Pro⎯Val-Asp-Lys⎯⎯OH

Title compound **28** was synthesized according to the general resin based procedure described above on a 50 µmol scale by incorporating the 1,4-disubstituted triazole **17**. The 5′-phosphoryl-ribofuranose intermediate was coupled to adenosine amidite **31**.[42] Purification of the crude residue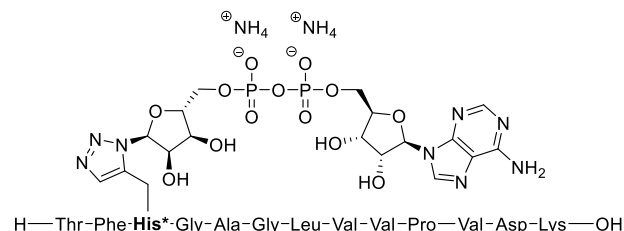 (50 µmol) by preparative HPLC (NH₄OAc buffer) and subsequent lyophilization yielded title compound **28** (33.2 mg, 17.7 µmol, 35%) as a fluffy white powder. The obtained spectra were in full accordance with previously reported experimental data.[35] **LC-MS** R_t = 4.42 min (10-50% MeCN/H₂O, TFA). **¹H NMR** (400 MHz, D₂O): δ 8.48 (s, 1H), 8.17 (s, 1H), 7.95pp (s, 1H), 7.27 − 7.16 (m, 3H), 7.10 (d, J = 8.0 Hz, 2H), 6.31 (d, J = 5.3 Hz, 1H), 6.07 (d, J = 5.8 Hz, 1H). **³¹P NMR** (162 MHz, D₂O): δ -10.32, -10.45, -10.70, -10.83. **HRMS** $[C_{76}H_{118}N_{22}O_{30}P_2 + 2H]^{2+}$ = 941.40011 found, 941.40025 calculated; $[C_{76}H_{118}N_{22}O_{30}P_2 + 3H]^{3+}$ = 627.93609 found, 627.93592 calculated.

N(π)-α-ADPr-His*: TF[H*]GAGLVVPVDK (H* = Triazolyl ADPr) (29).

H⎯⎯Thr-Phe-**His***-Gly-Ala-Gly-Leu-Val-Val-Pro⎯Val-Asp-Lys⎯⎯OH

Title compound **29** was synthesized according to the general resin based procedure described above on a 50 µmol scale by incorporating the 1,4-disubstituted triazole **19**. The 5′-phosphoryl-ribofuranose intermediate was coupled to adenosine amidite **31**.[41] Purification of half of the crude residue (25 µmol) by preparative HPLC (NH₄OAc buffer) and subsequent lyophilization yielded title compound **29** (11.9 mg, 6.37 µmol, 25%) as a fluffy white powder. **LC-MS** R_t = 4.38 min (10-50% MeCN/H₂O, TFA). **¹H NMR** (400 MHz, D₂O): δ 8.49 (s, 1H), 8.20 (s, 1H), 7.44 (s, 1H), 7.28 − 7.18 (m, 4H), 7.13 (d, J = 7.1 Hz, 2H), 6.35 (d, J = 5.2 Hz, 1H), 6.05 (d, J = 5.7 Hz, 1H). **³¹P NMR** (162 MHz, D₂O): δ -10.42, -10.54, -10.64, -10.77. **HRMS** $[C_{76}H_{118}N_{22}O_{30}P_2 + 2H]^{2+}$ = 941.39978 found, 941.40025 calculated; $[C_{76}H_{118}N_{22}O_{30}P_2 + 3H]^{3+}$ = 627.93585 found, 627.93592 calculated.

References

1. Huang, D. *et al.* Functional Interplay between Histone H2B ADP-Ribosylation and Phosphorylation Controls Adipogenesis. *Mol. Cell* **79**, 934-949.e14 (2020).
2. Schützenhofer, K., Rack, J. G. M. & Ahel, I. The Making and Breaking of Serine-ADP-Ribosylation in the DNA Damage Response. *Front. Cell Dev. Biol.* **9**, (2021).
3. Dantzer, F. & Santoro, R. The expanding role of PARPs in the establishment and maintenance of heterochromatin. *FEBS J.* **280**, 3508–3518 (2013).
4. Mashimo, M., Kato, J. & Moss, J. ADP-ribosyl-acceptor hydrolase 3 regulates poly (ADP-ribose) degradation and cell death during oxidative stress. *Proc. Natl. Acad. Sci.* **110**, 18964–18969 (2013).
5. Lüscher, B. *et al.* ADP-ribosyltransferases, an update on function and nomenclature. *FEBS J.* (2021) doi:10.1111/febs.16142.
6. Miwa, M. *et al.* A 13C NMR study of poly(adenosine diphosphate ribose) and its monomers: evidence of alpha-(1″ leads to 2′) ribofuranosy1 ribofuranoside risidue. *Nucleic Acids Res* **4**, 3997–4005 (1977).
7. Miwa, M. *et al.* The branching and linear portions of poly(adenosine diphosphate ribose) have the same alpha(1 leads to 2) ribose-ribose linkage. *J. Biol. Chem.* **256**, 2916–2921 (1981).
8. Lin, W., Amé, J.-C., Aboul-Ela, N., Jacobson, E. L. & Jacobson, M. K. Isolation and Characterization of the cDNA Encoding Bovine Poly(ADP-ribose) Glycohydrolase. *J. Biol. Chem.* **272**, 11895–11901 (1997).
9. Slade, D. *et al.* The structure and catalytic mechanism of a poly(ADP-ribose) glycohydrolase. *Nature* **477**, 616–620 (2011).
10. Jankevicius, G. *et al.* A family of macrodomain proteins reverses cellular mono-ADP-ribosylation. *Nat. Struct,. Mol. Biol.* **20**, 508–514 (2013).
11. Rosenthal, F. *et al.* Macrodomain-containing proteins are new mono-ADP-ribosylhydrolases. *Nat Struct Mol Biol* **20**, 502–507 (2013).
12. Moss, J., Tsai, S. C., Adamik, R., Chen, H. C. & Stanley, S. J. Purification and characterization of ADP-ribosylarginine hydrolase from turkey erythrocytes. *Biochemistry* **27**, 5819–5823 (1988).
13. Fontana, P. *et al.* Serine ADP-ribosylation reversal by the hydrolase ARH3. *Elife* **6**, 1–20 (2017).
14. Sharifi, R. *et al.* Deficiency of terminal ADP-ribose protein glycohydrolase TARG1/C6orf130 in neurodegenerative disease. *EMBO J.* **32**, 1225–1237 (2013).
15. Buch-Larsen, S. C. *et al.* Mapping Physiological ADP-Ribosylation Using Activated Ion Electron Transfer Dissociation. *Cell Rep.* **32**, 108176 (2020).
16. Fontana, P. *et al.* HPF1 completes the PARP active site for DNA damage-induced ADP-ribosylation. *Nature* (2020).
17. Burzio, L. O., Riquelme, P. T. & Koide, S. S. ADP ribosylation of rat liver nucleosomal core histones. *J. Biol. Chem.* **254**, 3029–3037 (1979).
18. Zhang, Y., Wang, J., Ding, M. & Yu, Y. Site-specific characterization of the Asp- and Glu-ADP-ribosylated proteome. *Nat Methods* **10**, 981–984 (2013).
19. Gagné, J.-P. *et al.* Quantitative site-specific ADP-ribosylation profiling of DNA-dependent PARPs. *DNA Repair* **30**, 68–79 (2015).
20. Leslie Pedrioli, D. M. *et al.* Comprehensive ADP-ribosylome analysis identifies tyrosine as an ADP-ribose acceptor site. *EMBO Rep.* **19**, e45310 (2018).
21. Vyas, S. *et al.* Family-wide analysis of poly(ADP-ribose) polymerase activity. *Nat. Commun.* **5**, 1–13 (2014).
22. Messner, S. *et al.* PARP1 ADP-ribosylates lysine residues of the core histone tails. *Nucleic Acids Res* **38**, 6350–6362 (2010).
23. Bartlett, E. *et al.* Interplay of Histone Marks with Serine ADP-Ribosylation. *Cell Rep.* **24**, 3488-3502.e5 (2018).
24. Hendriks, I. A., Larsen, S. C. & Nielsen, M. L. An advanced strategy for comprehensive profiling of ADP-ribosylation sites using mass spectrometry-based proteomics. *Mol. Cell Proteomics* **18**, 1010–1026 (2019).
25. Larsen, S. C., Hendriks, I. A., Lyon, D., Jensen, L. J. & Nielsen, M. L. Systems-wide Analysis of Serine ADP-Ribosylation Reveals Widespread Occurrence and Site-Specific Overlap with Phosphorylation. *Cell Rep.* **24**, 2493-2505.e4 (2018).
26. Voorneveld, J. *et al.* Synthetic α- and β-Ser-ADP-ribosylated Peptides Reveal α-Ser-ADPr as the Native Epimer. *Org. Lett.* **20**, 4140–4143 (2018).
27. Kliza, K. W. *et al.* Reading ADP-ribosylation signaling using chemical biology and interaction proteomics. *Molecular Cell* **81**, 4552-4567.e8 (2021).
28. Cohen, M. S. Catching mono- and poly-ADP-ribose readers with synthetic ADP-ribose baits. *Molecular Cell* **81**, 4351–4353 (2021).
29. Voorneveld, J. *et al.* Arginine ADP-Ribosylation: Chemical Synthesis of Post-Translationally Modified Ubiquitin Proteins. *J. Am. Chem. Soc.* **144**, 20582–20589 (2022).
30. van der Heden van Noort, G. J., van der Horst, M. G., Overkleeft, H. S., van der Marel, G. A. & Filippov, D. V. Synthesis of Mono-ADP-Ribosylated Oligopeptides Using Ribosylated Amino Acid Building Blocks. *J. Am. Chem. Soc.* **132**, 5236–5240 (2010).
31. Kistemaker, H. A. V. *et al.* Synthesis and Macrodomain Binding of Mono-ADP-Ribosylated Peptides. *Angew. Chem. Int. Ed.* **55**, 10634–10638 (2016).

32. Moyle, P. M. & Muir, T. W. Method for the Synthesis of Mono-ADP-ribose Conjugated Peptides. *J. Am. Chem. Soc.* **132**, 15878–15880 (2010).
33. Zhu, A. *et al.* Biomimetic α-selective ribosylation enables two-step modular synthesis of biologically important ADP-ribosylated peptides. *Nat. Commun.* **11**, 5600 (2020).
34. Li, L. *et al.* ADP-ribosyl-N3: A Versatile Precursor for Divergent Syntheses of ADP-ribosylated Compounds. *Molecules* **22**, 1346 (2017).
35. Minnee, H. *et al.* Mimetics of ADP-Ribosylated Histidine through Copper(I)-Catalyzed Click Chemistry. *Org. Lett.* **24**, 3776–3780 (2022).
36. Liu, Q. *et al.* A General Approach Towards Triazole-Linked Adenosine Diphosphate Ribosylated Peptides and Proteins. *Angew. Chem. Int. Ed.* **57**, 1659–1662 (2018).
37. Oppenheimer, N. J. Structural determination and stereospecificity of the choleragen-catalyzed reaction of NAD+ with guanidines. *J. Biol. Chem.* **253**, 4907–4910 (1978).
38. Boren, B. C. *et al.* Ruthenium-Catalyzed Azide−Alkyne Cycloaddition: Scope and Mechanism. *J. Am. Chem. Soc.* **130**, 8923–8930 (2008).
39. Empting, M. *et al.* "Triazole Bridge": Disulfide-Bond Replacement by Ruthenium-Catalyzed Formation of 1,5-Disubstituted 1,2,3-Triazoles. *Angew. Chem. Int. Ed.* **50**, 5207–5211 (2011).
40. Gold, H. *et al.* Synthesis of Sugar Nucleotides by Application of Phosphoramidites. *J. Org. Chem.* **73**, 9458–9460 (2008).
41. Kistemaker, H. A. V., Meeuwenoord, N. J., Overkleeft, H. S., Marel, G. A. van der & Filippov, D. V. Solid-Phase Synthesis of Oligo-ADP-Ribose. *Curr. Prot. Nucleic Acid Chem.* **64**, 4.68.1-4.68.27 (2016).
42. Hananya, N., Daley, S. K., Bagert, J. D. & Muir, T. W. Synthesis of ADP-Ribosylated Histones Reveals Site-Specific Impacts on Chromatin Structure and Function. *J. Am. Chem. Soc.* **143**, 10847–10852 (2021).
43. Štimac, A. & Kobe, J. An improved preparation of 2,3,5-tri-O-acyl-β-d-ribofuranosyl azides by the Lewis acid-catalysed reaction of β-d-ribofuranosyl acetates and trimethylsilyl azide: an example of concomitant formation of the α anomer by trimethylsilyl triflate catalysis. *Carbohydr. Res.* **232**, 359–365 (1992).
44. Yan, M., Lo, J. C., Edwards, J. T. & Baran, P. S. Radicals: Reactive Intermediates with Translational Potential. *J. Am. Chem. Soc.* **138**, 12692–12714 (2016).
45. Mao, Y. *et al.* Copper-catalysed photoinduced decarboxylative alkynylation: a combined experimental and computational study. *Chem. Sci.* **11**, 4939–4947 (2020).
46. Smith, J. M. *et al.* Decarboxylative Alkynylation. *Angew. Chem. Int. Ed.* **56**, 11906–11910 (2017).
47. Pradere, U., Roy, V., McBrayer, T. R., Schinazi, R. F. & Agrofoglio, L. A. Preparation of ribavirin analogues by copper- and ruthenium-catalyzed azide-alkyne 1,3-dipolar cycloaddition. *Tetrahedron* **64**, 9044–9051 (2008).
48. Voorneveld, J. *et al.* Molecular Tools for the Study of ADP-Ribosylation: A Unified and Versatile Method to Synthesise Native Mono-ADP-Ribosylated Peptides. *Chem. Eur. J.* **27**, 10621–10627 (2021).
49. Caron, J. *et al.* Squalenoyl Gemcitabine Monophosphate: Synthesis, Characterisation of Nanoassemblies and Biological Evaluation. *Eur. J. Org. Chem.* **2011**, 2615–2628 (2011).
50. Rack, J. G. M. & Ahel, I. A Simple Method to Study ADP-Ribosylation Reversal: From Function to Drug Discovery. *Methods Mol Biol* **2609**, 111–132 (2023).
51. Palazzo, L. *et al.* Processing of protein ADP-ribosylation by Nudix hydrolases. *Biochem.* **468**, 293–301 (2015).
52. Stevens, L. A. *et al.* The ARH and Macrodomain Families of α-ADP-ribose-acceptor Hydrolases Catalyze α-NAD+ Hydrolysis. *ACS Chem. Biol.* (2019) doi:10.1021/acschembio.9b00429.
53. Voorneveld, J. *et al.* Molecular Tools for the Study of ADP-Ribosylation: A Unified and Versatile Method to Synthesise Native Mono-ADP-Ribosylated Peptides. *Chem. Eur. J.* **27**, 10621–10627 (2021).
54. Rack, J. G. M. *et al.* (ADP-ribosyl)hydrolases: Structural Basis for Differential Substrate Recognition and Inhibition. *Cell Chem. Biol.* **25**, 1533-1546.e12 (2018).
55. Usuki, T. *et al.* Total synthesis of COPD biomarker desmosine that crosslinks elastin. *Chem. Commun.* **48**, 3233–3235 (2012).
56. Byrne, C., McEwan, P. A., Emsley, J., Fischer, P. M. & Chan, W. C. End-stapled homo and hetero collagen triple helices: a click chemistry approach. *Chem. Commun.* **47**, 2589–2591 (2011).